

AD-A267 723



FASTC-ID(RS)T-0731-92

# FOREIGN AEROSPACE SCIENCE AND TECHNOLOGY CENTER



DTIC  
ELECTE  
AUG 11 1993  
S C D

VERTICAL-TAIL AERODYNAMIC CONFIGURATION OF SPACE SHUTTLE ORBITER

by

Zhu Yikun



Approved for public release;  
Distribution unlimited.

93-18414



# **HUMAN TRANSLATION**

FASTC-ID(RS)T-0731-92 16 July 1993

MICROFICHE NR: 93C000455

VERTICAL-TAIL AERODYNAMIC CONFIGURATION OF SPACE  
SHUTTLE ORBITER

By: Zhu Yikun

English pages: 19

Source: Unknown; pp. 115-123

Country of origin: China

Translated by: Leo Kanner Associates  
F33657-88-D-2188

Requester: FASTC/TATV/Capt Stephen W. Stiglich, Jr.  
Approved for public release; Distribution unlimited.

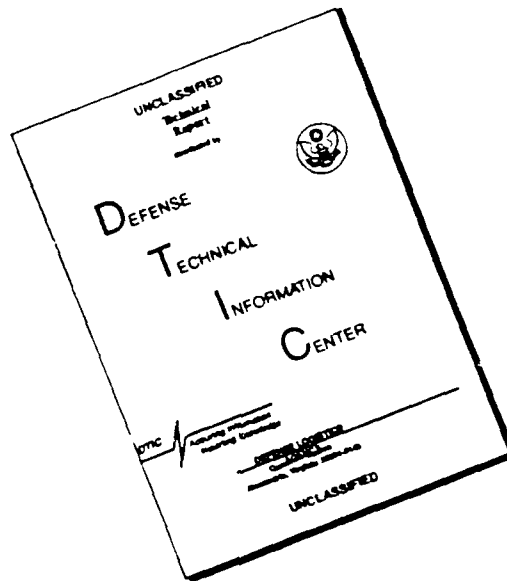
**DTIC QUALITY INSPECTED S**

Accession For	
NTIS CRA&I	<input checked="" type="checkbox"/>
DTIC TAB	<input type="checkbox"/>
Unannounced	<input type="checkbox"/>
Justification	
By	
Distribution /	
Availability Codes	
Dist	Avail and/or Special
A-1	

THIS TRANSLATION IS A RENDITION OF THE ORIGINAL FOREIGN TEXT WITHOUT ANY ANALYTICAL OR EDITORIAL COMMENT STATEMENTS OR THEORIES ADVOCATED OR IMPLIED ARE THOSE OF THE SOURCE AND DO NOT NECESSARILY REFLECT THE POSITION OR OPINION OF THE FOREIGN AEROSPACE SCIENCE AND TECHNOLOGY CENTER.

PREPARED BY:  
TRANSLATION DIVISION  
FOREIGN AEROSPACE SCIENCE AND  
TECHNOLOGY CENTER  
WPAFB, OHIO

# DISCLAIMER NOTICE



THIS DOCUMENT IS BEST  
QUALITY AVAILABLE. THE COPY  
FURNISHED TO DTIC CONTAINED  
A SIGNIFICANT NUMBER OF  
PAGES WHICH DO NOT  
REPRODUCE LEGIBLY.

#### GRAPHICS DISCLAIMER

All figures, graphics, tables, equations, etc. merged into this translation were extracted from the best quality copy available.

# VERTICAL-TAIL AERODYNAMIC CONFIGURATION OF SPACE SHUTTLE ORBITER

Zhu Yikun

Beijing University of Aeronautics and Astronautics

**Abstract:** From a discussion of the principle of the vertical-tail aerodynamic configuration of the Space Shuttle Orbiter in the preliminary design stage, and analysis of the vertical-tail aerodynamic configuration (including layout) of the present-day Space Shuttle Orbiter, the author clarified three possible modes of vertical-tail aerodynamic configuration of the Space Shuttle Orbiter, and the principal measures for the lateral-direction aerodynamic characteristics for an improved Space Shuttle Orbiter. These results have direct reference value on the aerodynamic configuration and the preliminary design on the exterior shape of the Space Shuttle Orbiter.

**Keywords:** Space Shuttle, aerodynamic configuration, vertical tail

## I. Introduction

The aerospace plane is an aerodynamic and astronautic flight vehicle, capable of multiple functions and dual maneuver modes

(maneuvers on the aircraft type aerodynamic surface and maneuver mode of rocket type reaction jet). At takeoff, the aerospace plane resembles a rocket or an aircraft, and in space orbit it acts like a spacecraft. During reentry, unpowered gliding for a horizontal landing, it operates like an aircraft. Requirements for complete repeat usage showed the contradiction between the hypersonic reentry unpowered gliding, as well as low and subsonic horizontal landing on a landing field. Thus, a serious challenge is posed to the aerodynamic configuration of the aerospace plane. In the paper, only an analysis and a discussion are made on the vertical-tail aerodynamic configuration of the aerospace plane in order to attain some concepts, line of reasoning, and conclusions for reference purposes at the preliminary design stage.

## II. Principle of Vertical-Tail Configuration of Aerospace Plane

During the middle and final stages of reentry flight for an aerospace plane, in particular flight resembling that of an aircraft during landing, in principle the vertical-tail aerodynamic configuration should be similar to the principle of the vertical-tail aerodynamic configuration of a hypersonic airplane. In the preliminary design of a hypersonic plane, in order to ensure a good motion stability in the lateral direction, it is generally that the airplane have translational and lateral static stability in various flight regimes. In other words, this requires that the yawing and rolling moment derivatives ( $m_y^{\beta}$ ,  $m_z^{\beta}$ ) of the aircraft to satisfy

$$m_y^{\beta} < 0 \quad (1)$$

and

$$m_x^{\theta} < 0$$

(2)

Translational static stability of an aircraft mainly derives from the stable yawing moment derivative  $(m_y^{\beta})_r < 0$  (Fig. 1) generated from the vertical tail. Therefore, Eq. (1) is the fundamental requirement of the vertical-tail aerodynamic configuration.

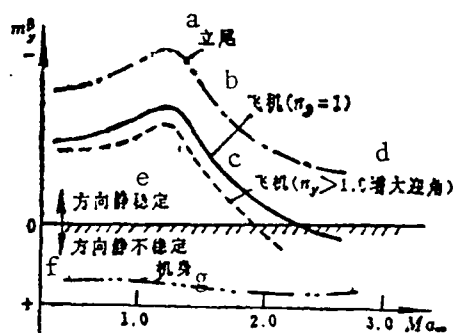


Fig. 1. Directional static stability of an aircraft

KEY: a - Vertical tail b - Aircraft  
c - Aircraft d - Increased angle of attack  
e - Directional static stability f - Directional static instability  
g - Fuselage

The aerodynamic configuration of the vertical tail should guarantee that Eq. (1) is satisfied under various flight regimes; however, there are great difficulties because of two main reasons as follows:

1. High-Mach-number effect: during hypersonic flight at increasing Mach number, the contribution made by the vertical tail to directional static stability is because of a rapid drop of lift curve slope of the vertical tail. However, the contribution to directional static instability (increasing with

increase in slenderness ratio of the forebody) made by the fuselage is nearly invariant with Mach number. This leads to a rapid decrease in directional static stability of the airplane (Fig. 1), and this regime may even occur to limit the maximum flight Mach number of the airplane because of an overly small  $-m_y^\beta$  value.

2. Large-angle-of-attack effect: during high-altitude flight at large angles of attack, the vertical tail is shadowed by the fuselage and an aircraft wing. The intensifying of the shock wave and the expansion wave at the fuselage nose and the aircraft wing leading edge, as well as separation vortices appearing at the wing-fuselage ensemble, will further reduce the contribution made by the vertical tail to directional stability [2-4].

Moreover, due to the factors of airflow separation above the wing surface and decreasing vertical tail effectiveness, there is also a reduction in the lateral static stability of the aircraft. In an extreme regime, even the translational and lateral static instabilities occur [3]; that is,  $m_y^\beta > 0$  and  $m_z^\beta > 0$  (Fig. 2).

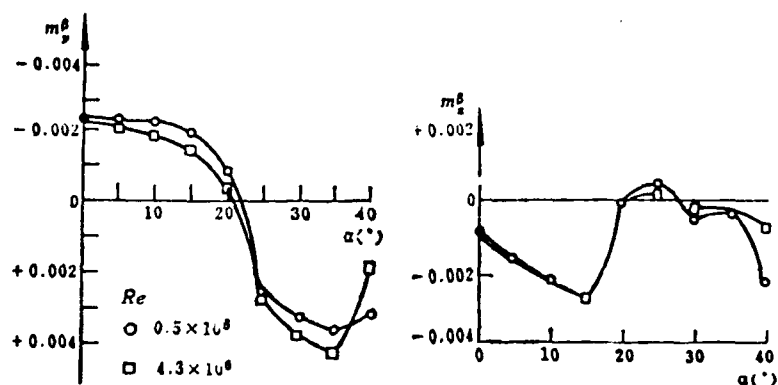


Fig. 2. Variation of lateral stability of airplane with angle of attack [3]



From the analysis of lateral motion stability of an airplane, the necessary condition for ensuring dutch roll stability is  $(m_y^{\beta})^* < 0$ , that is,

$$(m_y^{\beta})^* = m_y^{\beta} + m_x^{\beta} \frac{J_y}{J_x} \operatorname{tg} \alpha < 0 \quad (3)$$

In the equation,  $(m_y^{\beta})^*$  is called the dynamic parameter, or the effective direction-stability parameter;  $J_x$  and  $J_y$  are, respectively, the inertial moments of the fuselage about the  $ox$  and  $oy$  axes. For aircraft with  $J_y/J_x > 1.0$  and  $m_x^{\beta} < 0$ , according to Eq. (3), the requirements on  $m_y^{\beta}$  can be reduced. Even for just the regime in which  $m_y^{\beta} > 0$  and  $m_x^{\beta} > 0$  do not simultaneously occur, the lateral-direction motion stability will be seriously degraded. Using Eq. (1) as the design indicator will reduce the difficulty in vertical-tail configuration [3, 5].

### III. Analysis of Vertical-tail Aerodynamic Configuration and Performance of Aerospace plane

Below are the types for the vertical-tail aerodynamic configuration of the present-day aerospace plane (this means Orbiter, which is the term used in the following), and the second-generation aerospace plane; the concept of the latter has been proposed: central single vertical tail (Fig. 3); central up-and-down vertical tail (Fig. 4) [6]; wingtip double vertical tail (Fig. 5) [7-9]; V-shaped vertical tail (Fig. 6) [10]; and anomalous central single vertical tail (Fig. 7) [8], among other types. In the following, analyses are conducted on the performance of various configurations and types based on available data.

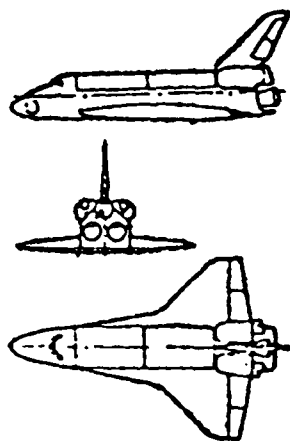


Fig. 3. U.S. Space Shuttle

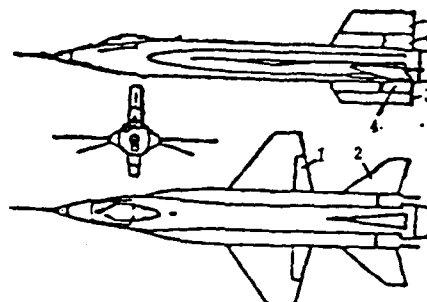


Fig. 4. U.S. X-15 aircraft  
LEGEND: 1 - Aileron  
2 - Flat tail 3, 5 - Upper and lower directional rudders 4 - speed-reducing flaps

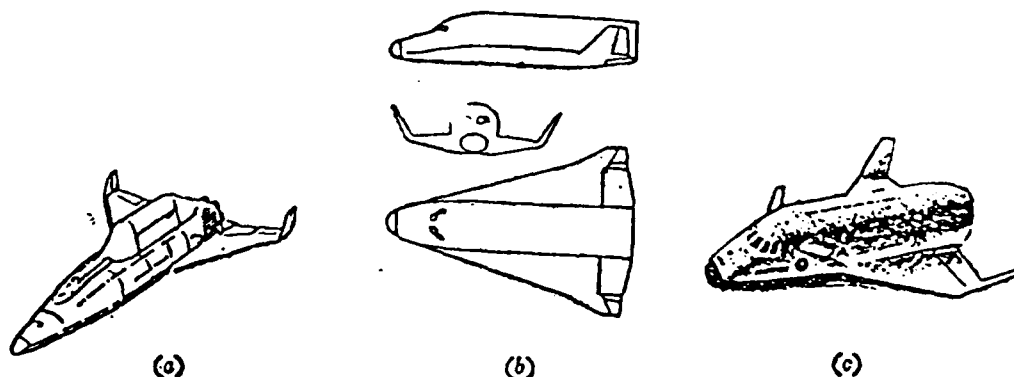


Fig. 5. Aerospace planes with wingtip double vertical-tail configurations: (a) - U.S. Shuttle-II Orbiter  
(b) Herms (France) (c) Hope (Japan)

#### 1. X-15 aircraft

Figs. 8 and 9 show the results of wind tunnel experiments and flight tests on  $m_y^0$ ,  $m_z^0$ , and  $(m_y^0)^*$  of the X-15 aircraft. The design of the vertical-tail configuration ensures that  $m_y^0 < 0$

is satisfied for all flight regimes. When  $Ma_\infty > 2.0$ ,  $m_x^2 > 0$ . However, since  $m_y^2 < 0$ , this still ensures that the requirements of  $(m_y^2)^* < 0$  are satisfied. The reasons why the directional-static stability is so good are because of the following.

a. Increase the face-to-face squareness ratio of the vertical tail  $A_v = S_v L_v / S b_A = 0.253$  (only the  $(A_v)_u$  of the upper vertical tail portion is equal to 0.138), which is much larger than the value  $A_v$  (approximately 0.05 to 0.09) [13] of the conventional aircraft class  $Ma_\infty = 2.0$ .

b. Adopt the above-and-below vertical tail configuration,  $(A_v)_l = 0.115$ . Since the interference due to shadowing and separation vortex of the fuselage and aircraft wing can be avoided, the aerodynamic efficiency is still high at large Mach number and large  $\alpha$ , thereby moderating the effect of a rapid drop in aerodynamic efficiency of the vertical tail.

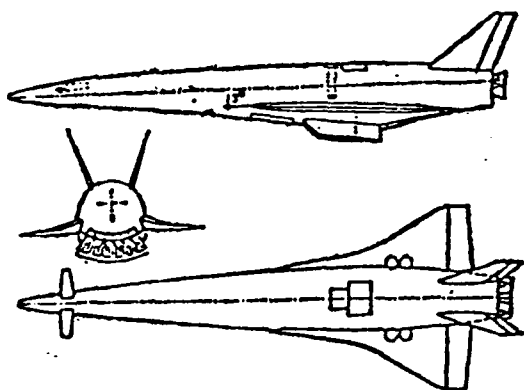


Fig. 6. Scheme of a hypersonic research craft

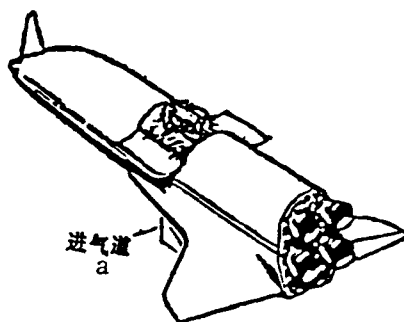


Fig. 7. British Hotol scheme  
KEY: a - Air intake duct

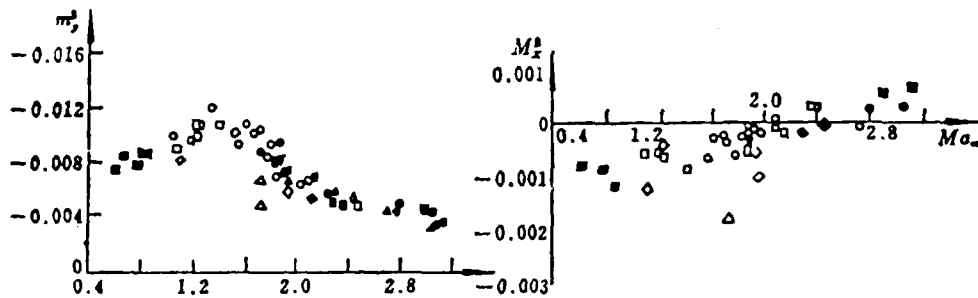


Fig. 8. Lateral-directional aerodynamic characteristics of X-15 craft [11]

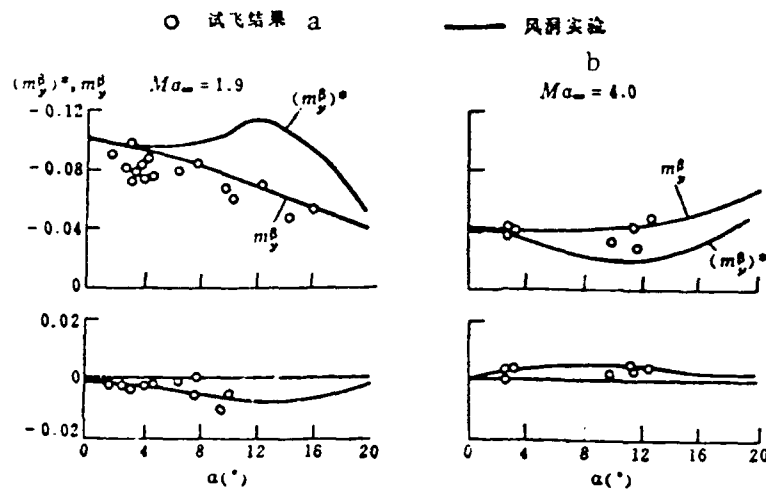
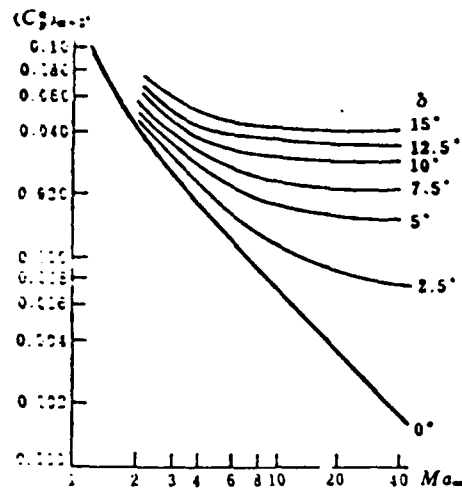


Fig. 9. Aerodynamic characteristics of X-15 craft  
KEY: a - Test flight results b - Wind tunnel experiments

c. By adopting the single-wedge wing tip (Fig. 4), its half-apex angle  $\delta = 5^\circ$ ; the relative thickness  $\bar{c} = 17.5$  percent. As verified in practice, during supersonic and especially hypersonic flight, this single-wedge wing type has good lift characteristics. Not only is the lift curve slope at the same  $Ma_\infty$  greater than for the flat wing type, but also the decrease in lift occurs at a slower rate with increase in  $Ma_\infty$  (Fig. 10) [14].



d. The speed-reducing flaps are skillfully installed on the lateral-wing surface in the up-and-down vertical tail; correspondingly, the wholly mobile type directional rubber at the exterior is adopted (Fig. 4). From Fig. 10, at the same  $Ma_{\infty}$ , the slope of the lift curve increases with increase in half-apex angle of the wing type, opening the speed-reducing flaps to the left and right corresponds to an increase in the half-apex angle; thus, this has apparent results in increasing the directional static stability of the vertical tail and the aircraft (Fig. 11). Therefore, at a high Mach number the speed-reducing flaps also have the function of aerodynamically increasing stability.

## 2. U.S. Space Shuttle

Fig. 13 shows the flight test results of the U.S. Space Shuttle along the reentry orbit  $m_y^\beta$ ,  $m_x^\beta$ , and  $(m_y^\beta)^*$ . The vertical-

tail configuration ensures that the flight along the reentry orbit satisfies the requirements of Eq. (3); only at low supersonic speeds and in the touchdown phase on the field is Eq. (1) satisfied. Otherwise, the relative face squareness ratio of the vertical tail will be too large (at present,  $A_v = 0.064$  for the U.S. Space Shuttle corresponds to the value of this aircraft in class  $Ma_\infty = 2.0$ ), so it is not feasible. Since only this kind of aircraft at  $Ma_\infty < 2.0$ , it has directional static stability. To ensure the quality of lateral-direction motion, the yawing reaction jet control system ceases to operate when  $Ma_\infty$  less than or equal to 1.

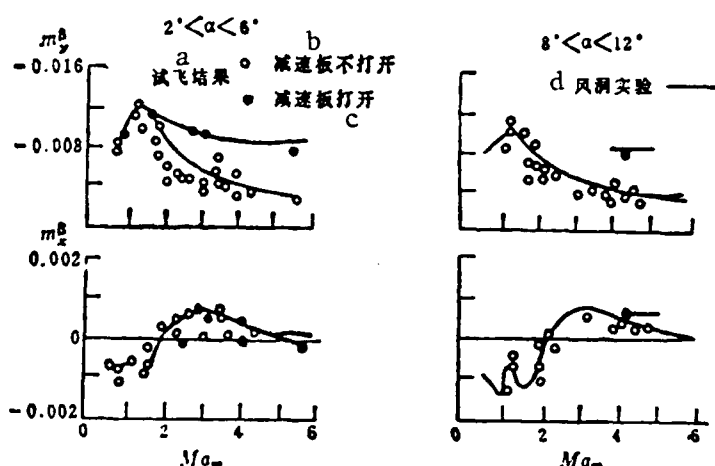


Fig. 11. Aerodynamic performance of speed-reducing flaps on X-15 aircraft

KEY: a - Flight test results b - Without opening speed-reducing flaps c - Opening speed-reducing flaps d - Wind tunnel experiments

The reasons why the U.S. Space Shuttle can satisfy the requirements in Eq. (3) are related to the fact that experience with the vertical configuration of X-15 craft was adequately applied. This is seen in the selection of wing types, as well as

the arrangement and application of speed-reducing flaps. In other words, the double-wedge-shaped wing type was selected so that the half-apex angle  $\zeta = 5^\circ$  at the leading edge, the maximum thickness is at 0.6 of the chord length, and the relative thickness is  $\bar{c} = 10.5$  percent. At the empennage, there is the directional rudder and the speed-reducing flaps; the equidirectional yawing at the rear section of the wing acts as a directional rudder. Different-directional yawing has the function of a speed-reducing flap. In the reentry process, the angle to which the speed-reducing flaps are opened is adjusted with variation in flight Mach number. When  $Ma_\infty > 10.0$ , the speed-reducing flaps are closed. When  $4.5 < Ma_\infty \leq 10.0$ , the open angle of the speed-reducing flaps is  $87.2^\circ$ . When  $1.0 < Ma_\infty < 4.0$ , the opening angle is  $55^\circ$ . When  $Ma_\infty < 0.9$ , the opening angle is  $25^\circ$ . It appears that opening of the speed-reducing flaps is important in making a contribution to directional static stability of the vertical tail, thus reducing directional instability at high Mach numbers. Data in Fig. 12 are the results of opening the speed-reducing flaps based on the foregoing. During subsonic landings, then the speed-reducing flaps have significant functions on the lift-to-drag ratio (Fig. 13). Such adjustments of the speed-reducing flaps are favorable to the lateral- and longitudinal-direction aerodynamic characteristics of aircraft.

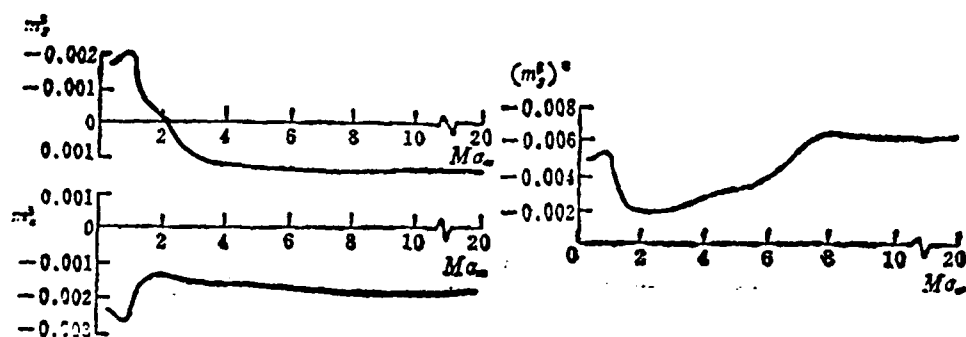


Fig. 12. Lateral-directional aerodynamic characteristics of the U.S. Space Shuttle [15]

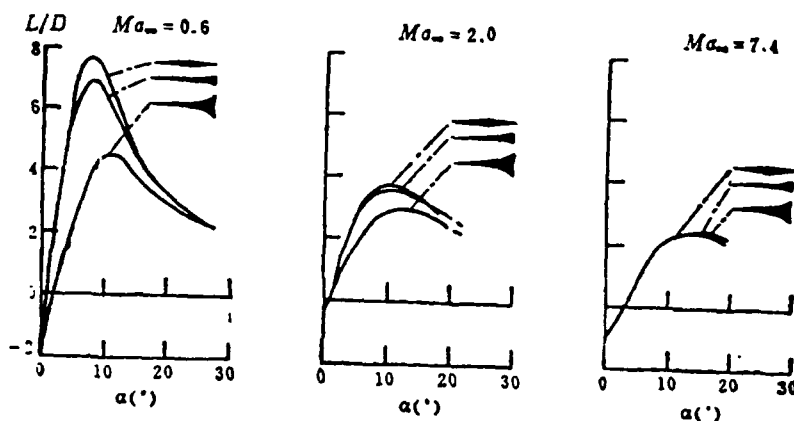


Fig. 13. Effect on lift-to-drag ratio of aerospace plane due to opening the speed-reducing flaps [17]

### 3. Wingtip double-vertical tails configuration

During the development of the U.S. Space Shuttle, studies were made of the wingtip double-vertical tails configuration. Fig. 14 shows the variations in  $m_y^\beta$ ,  $m_x^\beta$ , and  $(m_y^\beta)^*$  with angle at  $Ma_\infty = 7.4$  for different vertical-tail configurations; the wingplane is delta-shaped. From the figure, in any regimes,



all  $m_y^B$  are greater than zero, but  $m_x^B$  is less than 0. The wingtip double-vertical tails and the absence of a vertical tail satisfy the condition of  $(m_y^B)^* < 0$  at hypersonic speeds and large  $\alpha$ . In the regimes of low supersonic speeds or subsonic speeds at small angles of attack ( $\alpha = 0$ ), the performance of the wingtip double-vertical tails is not as good as for the case of the central single vertical-tail type [15]. The reason is that there is no interference with the positive lift between the central single vertical tail and the fuselage for the case of the wingtip double-vertical tails, and there is no contribution to the lateral stability. The force arm  $L_y$  of the double-vertical tails is shorter; with the same vertical tail area  $S_v$ , the aerodynamic efficiency will be somewhat lower. In addition, the interference between the wingtip double-vertical tails and the wing surface will degrade the flow in the wingtip region, thus advancing the separation with the appearance of pitch-up moment (Fig. 16). Therefore, the wingtip double tails exhibit low efficiency at low supersonic speeds or subsonic speeds.

Through systems research on various vertical-tail configurations to ensure and satisfy the required equilibrium, stability, and maneuverability needed in the reentry phase and on the principle of minimum structural weight, and the emphasis is placed on the low supersonic and subsonic landing phases, finally, the central single-vertical-tail type was selected for the U.S. Space Shuttle. However, with advances in powered-control techniques, it is possible to further moderate the

requirements on directional static stability during subsonic flight. Therefore, in the reentry transitional phase of the present-day U.S. Space Shuttle (transition from large angles of attack and low-speed pressure to small angles of attack and high-speed pressure, corresponding to  $Ma_\infty = 15 \sim 1.5$ ), that the weak points of the central single vertical tail and the directional rudder play nearly no role, is very significant. Mainly, the directional maneuver and balance rely on joint functioning of the aerodynamic control surfaces of the ailerons and the reaction type jet control system. The selection of the wingtip small-dimensional double-vertical tails and the splitting type control surfaces (Fig. 17) can overcome the above-mentioned weak points, and the area is less than one-quarter of the area for the original central single vertical tail. This configuration type does not have any inherent directional static stability (Fig. 18); the required stability in lateral motion is provided by powered control techniques (through aerodynamic control surfaces and jet control systems). However, this arrangement is low in structural weight and high in directional-control capability (this arrangement can advance the closing of the jet control system with a savings of fuel and avoidance of unfavorable interference with the airstream. This reduces reliance on ailerons with directional control equilibrium, therefore reducing indeterminacy in designing the control system, among other factors), and also being beneficial to the release of the effective payload from the cargo bay (without hindrance from the

central single vertical tail), among other advantages. Therefore, the wingtip double-vertical-tail configuration attracts attention in designing the next-generation aerospace plane.

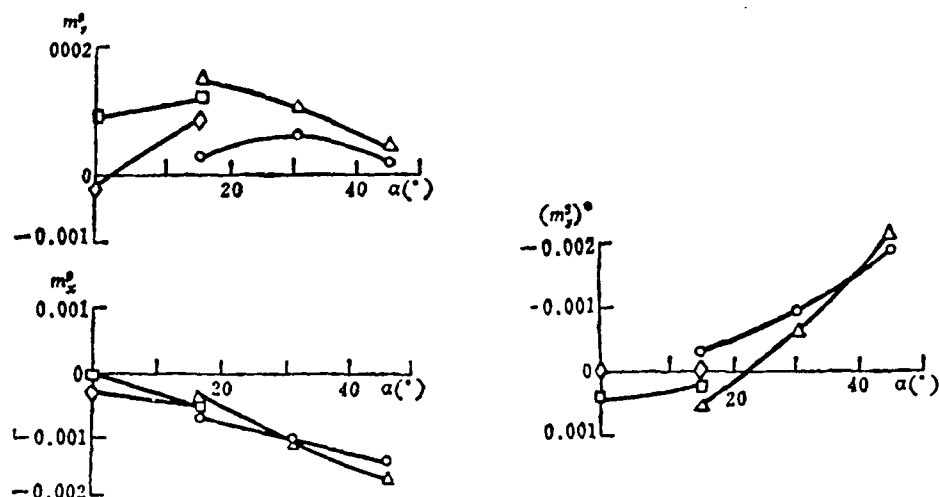


Fig. 14. Lateral stability of different vertical-tail configuration at hypersonic speeds [16]

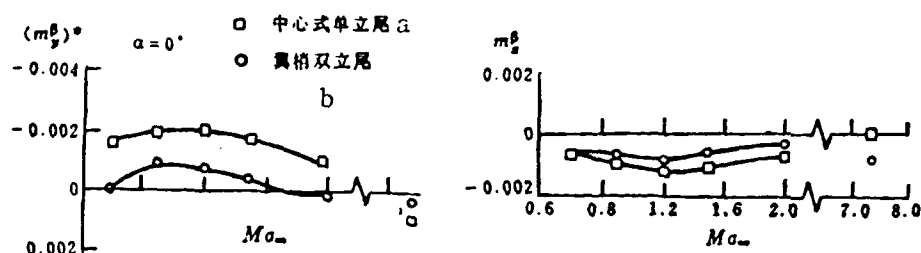


Fig. 15. Lateral stability of two vertical-tail configurations at low supersonic speeds and subsonic speeds [16]

KEY; a - Central type single vertical tail  
b - Double vertical tail

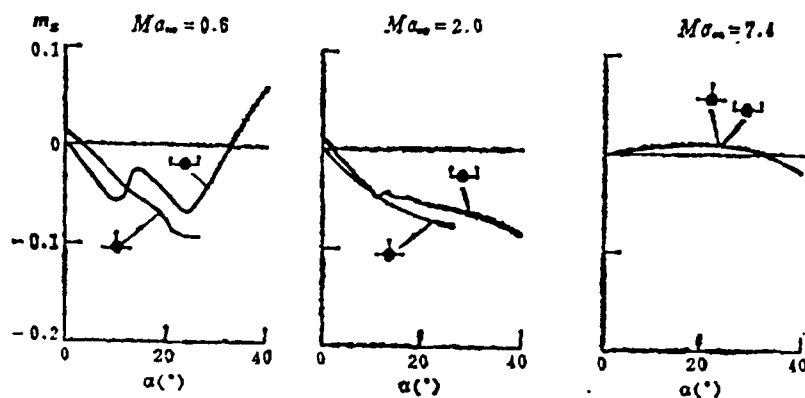


Fig. 16. Longitudinal stability of two vertical tail configurations [16]

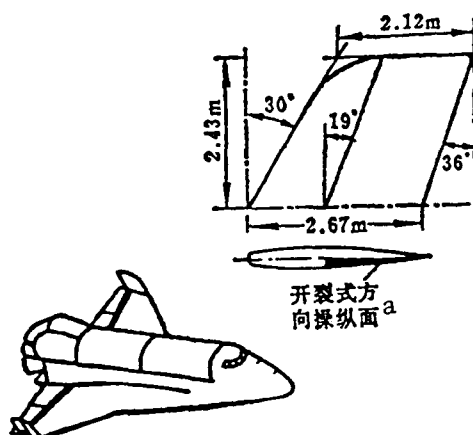


Fig. 17. One of the improved schemes for the U.S. Space Shuttle (wingtip double-vertical tails) [17]  
KEY: a - Splitting type directional control surface

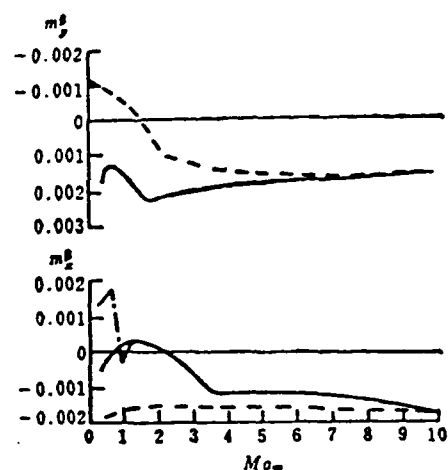


Fig. 18. Lateral stability of two vertical tail configuration for U.S. Space Shuttle

Fig. 19. shows the scheme of a single-stage transport orbiter (SSTO). The figure shows two configuration types of vertical tail. Since the position of the center of mass is quite rearward (located at  $0.71 \sim 0.74$ , or  $0.76 \sim 0.78$  of the fuselage length, determined by the effective payload size. For the

present-day U.S. Space Shuttle and the aircraft for the  $Ma_\infty = 2.0$  class, the locations of the mass center are, respectively,  $0.65 \sim 0.675$  and  $0.52 \sim 0.54$ ), even if the central single vertical tail layout is selected since the vertical tail force arm is too small, it is not only difficult to ensure directional static stability during the reentry phase, it is even difficult to ensure that  $(m_y^B)^* < 0$  can be satisfied (Fig. 19(b)). In such a case it is better to adopt the wingtip double-vertical-tail configuration. To remedy the insufficiency of too low subsonic landing control effectiveness by the wingtip control surfaces, a lateral force flap can be installed beneath the shuttle nose, to be opened during landing (Fig. 19(a)).

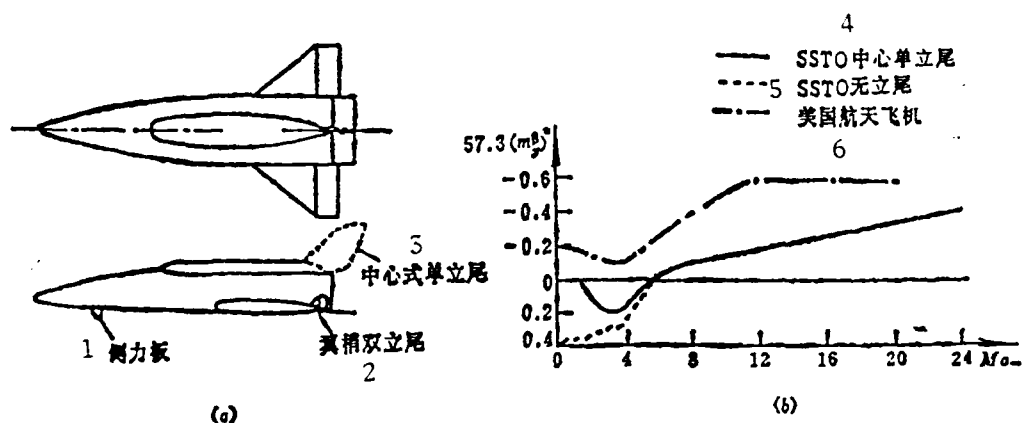


Fig. 19. Performance of  $(m_y^B)^*$  for an SSTO scheme [18]  
 KEY: 1 - Lateral force flap 2 - Wingtip double vertical tails 3 - Central single vertical tail  
 4 - SSTO central single vertical tail 5 - SSTO in the absence of vertical tail 6 - U.S. Space Shuttle

In the British Hotal scheme (Fig. 7) the anomalous central single vertical tail (directional control surface) was selected because in this layer the force arm is larger. Obviously, this

layout is unable to have any function of static stability along any direction, exhibiting only the function of directional control equilibrium. It is required to satisfy the directional trimming, control, and artificial increase in stability (among other factors) in an overall consideration. Possibly, the yawing reaction type jet control system may operate ultimately.

#### IV. Results

The vertical tail aerodynamic configuration of the Space Shuttle is considered for completion of reentry flight. Possibly, there are three modes for the layout principle.

1. It is required to satisfy Eqs. (1) and (3), and the X-15 craft mode. This is the conventional mode of vertical tail configuration of supersonic aircraft.

2. It is required to satisfy Eq. (3); only at the low supersonic and subsonic landing modes is it required to satisfy Eq. (1), as the present mode of the U.S. Space Shuttle. This is a good method based on the situation of techniques then available to partially break with the conventional mode in solving a concrete problem.

3. It is required to partially satisfy Eq. (3), but not to entirely satisfy Eq. (1); this is the mode selected at present in the concept of the second-generation and third-generation aerospace planes. This approach fully breaks with the conventional mode, and moderates the requirements of directional static stability throughout the speed range. Thus, at the outset it is required to rely on advanced integrated design systems and

primary control techniques in preliminary design; however, these techniques still call for practical verification before being put into execution.

#### REFERENCES

1. Yeager, C. M. et al, translated by Zhang Xichun and Wu Wenzheng, Feiji Sheji [Aircraft Design], National Defense Industry Publishing House, 1987, pp. 227-235.
2. Young J C, Underwood J M, et al. NASA CP-2283, 1983, 209~263
3. Chambers J R, Anglin L. NASA TN D-5361, 1967
4. Walker H J, Wolowicz C H. NASA TM X-287, 1965
5. Gamble J D, Cooke D R, et al. NASA CP-2283, 1983, 264~294
6. Weil J. NASA TN D-1278 1952
7. Holloway P F, Talag T A. IAF-87-188 1987
8. Speer Maj T E, Hoyt Capt A R. AIAA 15th Aerodynamic Testing Conference. 1988, 1~10
9. Davis N W. Aerospace America, 1988, 26, (3)22~25
10. Kandebo S W. Aviation Week & Space Technology 1988, 129, (14)38~39
11. Seckel E. Stability and Control of Airplane and Helicopter. Academic Press, 1964
12. Walker H J, Wolowicz C H. NASA TM X-714 1965
13. Roskam J. Airplane Design Part II. Roskam Aviation and Engineering Corporation 1985, 200
14. McLellen C H. NACA RM L54F21, 1954
15. Surber T E, Olsen D C. J Spacecraft 1978, 15(1), 40~47
16. Peterson V L, Katzen E D, Axelson J A, et al. NASA Space Shuttle Technology Conference, Vol 1, 1971, 311~373
17. Powell R W, Freeman Jr D C. J Spacecraft 1985, 22(5), 536~540
18. Freeman Jr D C, Powell R W. J Spacecraft 1980 17(4), 311~315

DISTRIBUTION LIST

DISTRIBUTION DIRECT TO RECIPIENT

<u>ORGANIZATION</u>	<u>MICROFICHE</u>
B085 DIA/RIS-2FI	1
C509 BALLOC509 BALLISTIC RES LAB	1
C510 R&T LABS/AVEADCOM	1
C513 ARRADCOM	1
C535 AVRADCOM/TSAROOM	1
C539 TRASANA	1
Q592 FSTC	4
Q619 MSIC REDSTONE	1
Q008 NTIC	1
Q043 AFMIC-IS	1
E051 HQ USAF/INET	1
E404 AEDC/DOF	1
E408 AFWL	1
E410 ASDTC/IN	1
E411 ASD/FTD/TTIA	1
E429 SD/IND	1
P005 DOE/ISA/DDI	1
P050 CIA/OCR/ADD/SD	2
1051 AFTT/LDE	1
PO90 NSA/CDB	1
2206 FSL	1

Microfiche Nbr: FTD93C000455  
FTD-ID(RS)T-0731-92